Theoretical study of effect of carrier-density-dependent internal loss in the optical confinement layer (OCL)on the characteristic temperature of semiconductor – quantum dot (QD) lasers .

Dr. Kadhim A. Hubeatir
Assist. Prof.

Dr. Mohammed A. Mahde
Lecturer

Mr.. Razi J. Al-Azawi
Lecturer

Abstract

Internal optical loss in a QD laser couples the confined-carrier level occupancy in QDs to the free-carrier density in the OCL. Due to this coupling, which is controlled by the threshold condition, the free-carrier density is increased and more temperature-sensitive, and also the confined-carrier level occupancy becomes temperature-dependent. As a result, the characteristic temperature of a laser is considerably reduced. Carrier-density-dependent internal loss also sets an upper limit for operating temperatures of a QD laser and constrains the shallowest potential well depth and the smallest tolerable size of a QD at which the lasing can be attained. The dependences of the characteristic temperature, maximum operating temperature, and shallowest potential well depth on the parameters of the structure are obtained. At the maximum operating temperature or when any parameter of the structure is equal to its critical tolerable value, the characteristic temperature reduces to zero.

I. Introduction

Temperature-stable diode lasers are highly desired for optical fiber telecommunication systems. The temperature dependence of the threshold current density of a semiconductor laser can be expressed as [1].

$$j_{th} \propto \exp\left(\frac{T}{T_0}\right),$$

where $T0$ is the characteristic temperature – a very important and widely accepted figure of merit of semiconductor lasers defined as

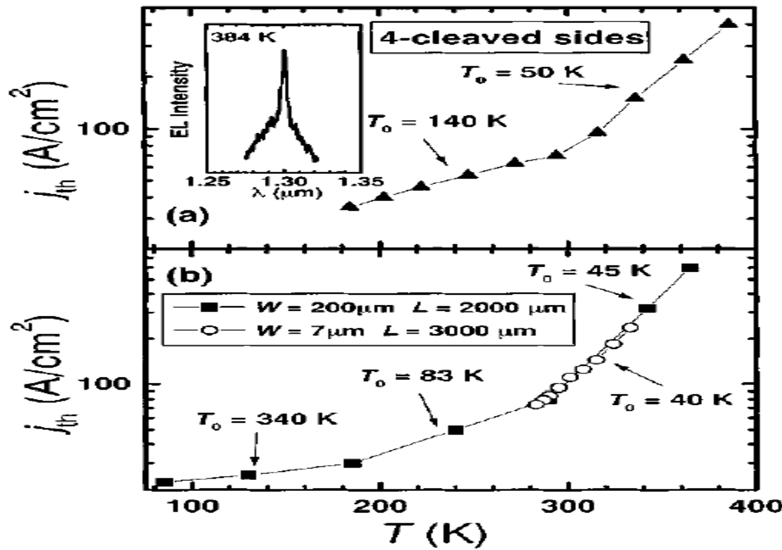

Fig. 1. Temperature dependence of the threshold current density of a structure with
four-cleaved sides (a) and a stripe device (b). The stripe width (*W*) and length (*L*).

$$T_0 = \left(\frac{\partial \ln j_{\text{th}}}{\partial T} \right)^{-1} . \qquad (2)$$

The less temperature-sensitive is jth, the higher is $T0$ (see Fig. 1) .

High temperature stability of operation is anticipated from semiconductor quantum dot (QD) lasers [2]. This advantage stems from a discrete energy spectrum of carriers in dots as shown in Fig. 2 [1].

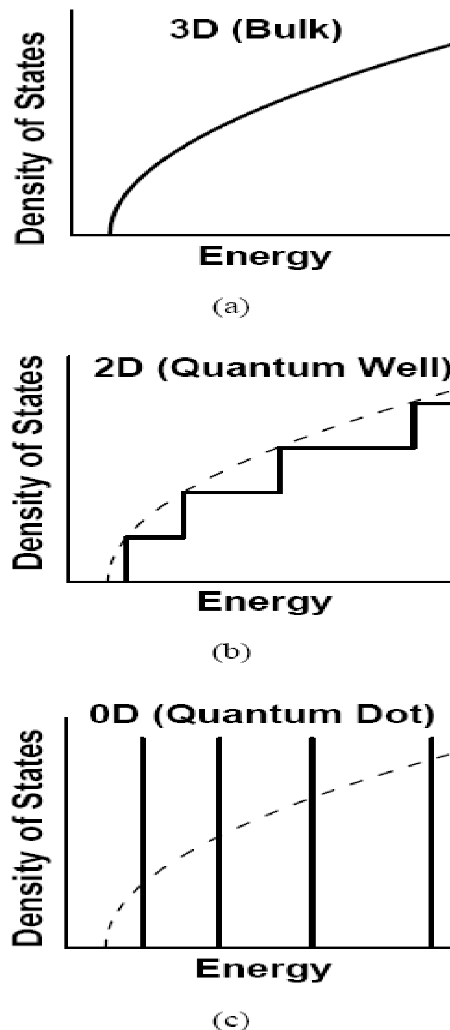

Fig. 2. Density of states in materials of different dimensionality: (a) 3D (bulk), (b) 2D (QW), and (c) 0D (QD).

Improved temperature stability of j_{th} has been first demonstrated by placing QW lasers in strong magnetic fields to achieve three-dimensional confinement of carriers . In an ideal QD laser, the threshold current density jth should remain unchanged with the temperature and the characteristic temperature should be infinitely high [2]. This would be the case if the overall injection current went into QDs, and the recombination current in QDs would be temperature-independent. In actual QD lasers, carriers are first injected from the cladding layers into the optical confinement layer (OCL) (which includes the wetting layer), and then captured into QDs. The presence of carriers in the

OCL results in recombination therein. Hence the recombination processes both in QDs and in the OCL control *j*th and its *T*-dependence [1, 2]:

$$j_{\text{th}} = j_{\text{QD}} + j_{\text{OCL}}, \tag{3}$$

$$\frac{1}{T_0} = \frac{j_{\text{QD}}}{j_{\text{QD}} + j_{\text{OCL}}} \frac{1}{T_0^{\text{QD}}} + \frac{j_{\text{OCL}}}{j_{\text{QD}} + j_{\text{OCL}}} \frac{1}{T_0^{\text{OCL}}}, \tag{4}$$

where *j*QD and *j*OCL are the components of *j*th associated with the recombination in QDs and in the OCL, respectively, and T_0^{QD} and T_0^{OCL} are defined similarly to *T*0 but for *j*QD and *j*OCL, respectively. The components of *j*th are given as

$$j_{\text{QD}} = \frac{eN_S}{\tau_{\text{QD}}} f_n f_p, \qquad j_{\text{OCL}} = ebBnp, \tag{5}$$

where *N*S is the surface density of QDs, τ_{QD} is the spontaneous radiative recombination time in QDs, *f*n and *f*p are the confined-electron and -hole level occupancies in QDs at the lasing threshold, *b* is the OCL thickness, *B* is the radiative constant for the OCL material, and *n* and *p* are the free-electron and -hole densities in the OCL at the lasing threshold.
The *T*-dependence of free-carrier densities, *n* and *p*, acts as the major source of such dependence of *j*th [1,2]. Thus, when the carrier distribution (below and at the lasing threshold) is described by the equilibrium statistics (relatively high *T*), *n* and *p* depend exponentionally on *T*

$$n = n_1 \frac{f_n}{1 - f_n} = N_c^{\text{OCL}} \exp\left(-\frac{E_n}{T}\right) \frac{f_n}{1 - f_n}, \tag{6}$$

Where

$$n_1 = N_c^{\text{OCL}} \exp\left(-E_n/T\right), \; N_c^{\text{OCL}} = 2\left(m_c^{\text{OCL}} T / 2\pi\hbar^2\right)^{3/2}$$

$m_C^{OCL}$is the electron effective mass in the OCL, T is the temperature measured in units of energy, and En is the carrier excitation

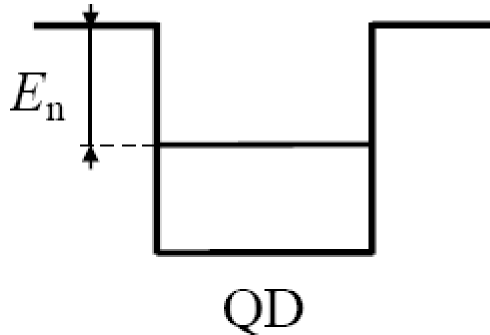

Fig.3. Energy of the carrier excitation from a QD to the OCL.

energy from a QD to the OCL [see Fig.3 and also the inset in Fig. 10(a)]. The temperature T here is measured in units of energy. The equation for p is similar to eq. (6).
Different factors can contribute to the T-dependence of the confined-carrier level occupancies in QDs, fn,p, thus causing the temperature-dependence of the recombination current density in QDs, j_{QD}, and making T_0^{QD} finite. violation of charge neutrality in QDs (fn ≠ fp) was shown to be such a factor.

II. Carrier-density-dependent internal loss in the waveguide

Here we study the effect of carrier-density-dependent internal optical loss in the OCL on the temperature dependence of jth. As in other injection lasers [3–8], such a loss can strongly affect the temperature stability of QD lasers. This work is based on [3], where jth has been calculated in the presence of the carrier-density-dependent internal loss. To neatly clarify the effect of internal loss, the charge neutrality [separately in QDs (fn = fp) and in the OCL ($n = p$)] is assumed here. In general, several mechanisms can contribute to the internal loss, such as free-carrier absorption in the OCL and scattering at rough surfaces and imperfections in the waveguide [3]. All these mechanisms can be conveniently grouped into the two categories – one dependent on the carrier density in the OCL and the other independent. Hence, the overall internal loss coefficient αint can be written as a sum of two components – one constant (αint) and the other increasing with the carrier density n,

$$\alpha_{int} = \alpha_0 + \sigma_{int} n , \quad (7)$$

where σint is the effective cross section for the internal absorption loss processes [3].With eq. (7), the lasing threshold condition (equality of the gain to the loss) can be written as

$$g^{max}(2f_n - 1) = \beta + \alpha_0 + \sigma_{int} n \quad (8)$$

where g^{max} is the maximum (saturation) gain [7], $\beta = (1/L)\ln(1/R)$ is the mirror loss, *L* is the cavity length, and *R* is the facet reflectivity.In the absence of the carrier-density-dependent internal loss (σint= 0), the level occupancy is immediately obtained from eq. (8) to be independent of temperature,

$$f_n^{const} = \frac{1}{2}\left(1 + \frac{\beta + \alpha_0}{g^{max}}\right). \quad (9)$$

Hence, j_{QD} = const(*T*) and $T_0^{QD}=\infty$ in this case.As seen from eq.(8), the carrier-density-dependent internal loss couples *n* and *f*n and, in view of the temperature dependence of *n*, makes *f*n and j_{QD} also temperature dependent. Thus, T_0^{QD}becomes finite.
The following expression for *f*n [which is easily found from eqs. (6) and (8)] has been
derived in [4] [see eq. (9) there in]:

$$f_n = \frac{1}{2}\left(1 + f_n^{const} - \frac{1}{2}\frac{\sigma_{int} n_1}{g^{max}}\right) - \sqrt{\frac{1}{4}\left(1 + f_n^{const} - \frac{1}{2}\frac{\sigma_{int} n_1}{g^{max}}\right)^2 - f_n^{const}} \quad (10)$$

where fn ^{const} is given by eq. (9).

As seen from eq. (10), the temperature dependence of *f*n stems from such dependence of *n*1 [see eq. (6)]. In what follows, a possible *T*-dependence of σint is neglected compared to the exponential *T*-dependence of *n*1. Fig. 4 shows the temperature-dependence of the

confined carrier level occupancy in QDs (right axis) given by eq. (10), the free-carrier density in the OCL and the internal loss (left axis) obtained from eqs. (8) and (10). In view of a linear character of eq. (8), the curve for all these quantities, *f*n, *n*, and α_{int}, is the same, and the vertical axes for them are obtained by a simple rescaling from one another. In the presence of the carrier-

density-dependent internal loss, the confined-carrier level occupancy increases with temperature

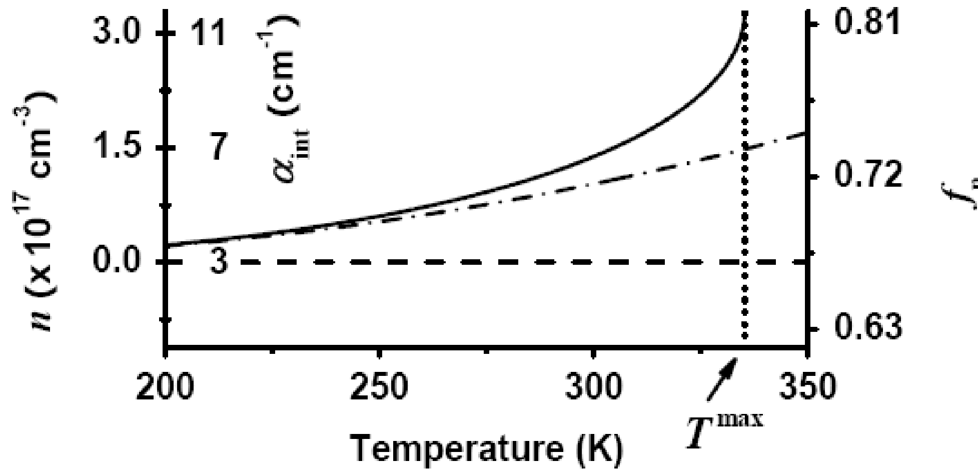

Fig. 4. Confined-carrier level occupancy in QDs, *f*n (right axis), free-carrier-densityin the OCL, *n*, and internal loss αint (left axis) against temperature in the presence of the carrier-density-dependent internal loss (solid curve). The horizontal dashed line indicates α_{int} and *f*n in the absence of the carrier-density-dependent internal loss. The dash-dotted curve shows *n* in the absence of the carrier-density-dependent internal loss. The vertical dotted line marks the maximum operating temperature T^{max} in the presence of the carrier-density-dependent internal loss [see eq. (14)].: the mean size of QDs
a = 150 Å, the root mean square (RMS) of relative QD size fluctuations δ = 0.05 (Gaussian distribution is assumed), the OCL thickness *b* = 0.28 µm, the surface density of QDs

*N*S = 6.11×10^{-10} cm^{-2}, the constant component of internal loss α_0 = 3 cm^{-1}, the cross section of internal loss $\sigma_{int} = 2.67 \times 10^{-17}$ cm^2, the cavity length *L* = 1.628 mm, and the mirror loss β = 7 cm^{-1}.

Both *f*n and *n* are increased compared to their values in the absence of such a loss (the latter are given by the horizontal dashed line and dash-dotted curve, respectively). The vertical dotted line marks the maximum operating temperature $T^{max}$of a QD laser in the presence of the carrier-density-dependent internal loss.
GaInAsP/InP heterostructure lasing near 1.55 µm is considered , the parameters are indicated in the caption to Fig. 4 .

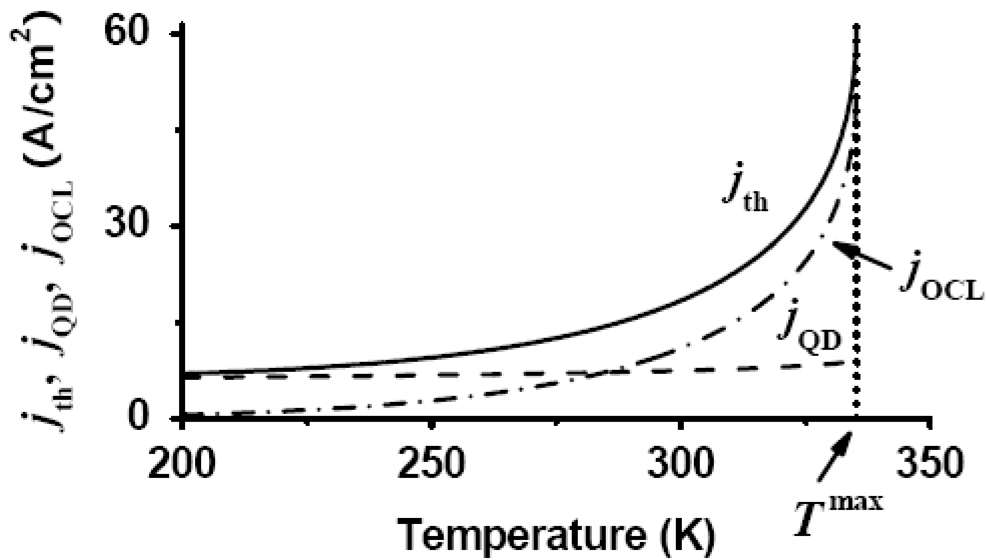

Fig. 5. Threshold current density jth (solid curve) and its components j_{QD} (dashed curve) and j_{OCL} (dash-dotted curve) against temperature. The vertical dotted line marks the maximum operating temperature T^{max}.

It is seen from eq. (10) that, in order to have a positive real fn, the expression in the square root should be larger than or equal to zero.

Implementing this condition gives the critical value of fn and hence the critical values of structure parameters. While in the absence of carrier density-dependent internal loss [5], the critical value of fn is unity, the critical value of fn in the presence of such a loss is smaller than unity. Therefore, the carrier-density-dependent internal loss narrows the range of possible values of the structure parameters, within which lasing action in a QD laser can be attained. The threshold current density jth and its components j_{QD} and j_{OCL} associated with the recombination in QDs and in the OCL are shown in Fig. 5 [4,5]. Although j_{QD} becomes temperature-dependent in the presence of the carrier- density- dependent internal loss, its temperature dependence is much weaker than that of j_{OCL}. Correspondingly, T_0^{QD} is much higher than T_0^{OCL} (Fig. 6). While j_{OCL} is smaller than j_{QD} at relatively low temperature, it increases with temperature much faster than jQD does, and surpasses the latter at relatively high temperature (Fig. 5). It is the recombination in the OCL that is a major obstacle to a superior performance of QD lasers at room temperature or

III. Characteristic temperature in the presence of carrier-density-dependent internal loss

Assuming the charge neutrality in QDs ($f_n = f_p$) and using (5), we have

$$\frac{1}{T_0^{QD}} = \frac{2}{f_n}\frac{\partial f_n}{\partial T} . \qquad (11)$$

The carrier-density-dependent internal loss formally plays a role similar to that of violation of charge neutrality in QDs [6, 7], affecting the characteristic temperature T_0 via its effect on the level occupancy f_n.

Putting eqs. (10) into (11) yields the following expression for T_0^{QD} :

$$\frac{1}{T_0^{QD}} = \frac{1}{\sqrt{\frac{1}{4}\left(1+f_n^{const}-\frac{1}{2}\frac{\sigma_{int}n_1}{g^{max}}\right)^2 - f_n^{const}}}\frac{\sigma_{int}n_1}{2g^{max}}\left(\frac{3}{2}\frac{1}{T}+\frac{E_n}{T^2}\right). \qquad (12)$$

The carrier-density-dependent internal loss also alters the temperature dependence of j_{OCL} since the free-carrier density at the lasing threshold is strongly affected. The expression for T_0^{OCL} in this case can then be expressed as

$$\frac{1}{T_0^{OCL}} = \frac{3}{2}\frac{1}{T} + \frac{2E_n}{T^2} + \frac{1}{1-f_n}\frac{1}{T_0^{QD}} . \qquad (13)$$

The sum of the first two terms in the right-hand side of eq. (13) presents the reciprocal of T_0^{OCL} in the absence of the carrier-density dependent internal loss [6]. As seen from eq. (13), T_0^{OCL} is reduced in the presence of such a loss. T_0^{QD} and T_0^{OCL} are shown versus temperature in Fig. 6. With increasing temperature, the effect of the carrier-density-dependent internal loss becomes

more strongly manifested and hence T_0^{QD} (the solid curve) decreases. This is in contrast to the effect of charge neutrality violation in QDs, which is suppressed with increasing temperature —T_0^{QD} controlled by the latter effect increases with temperature [6].

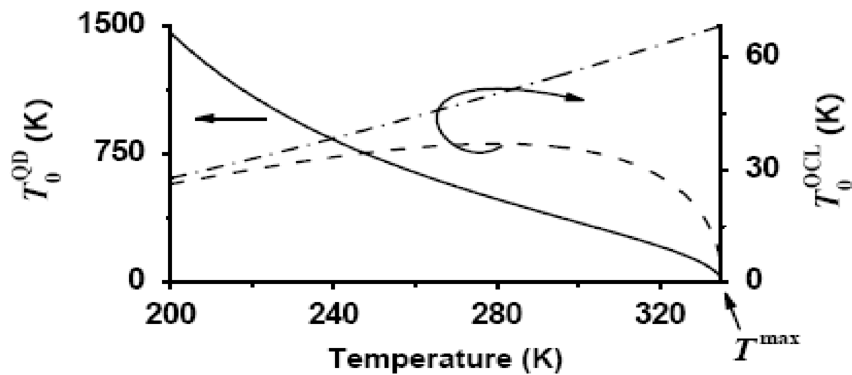

Fig. 6.

T_0^{QD} (solid curve, left axis) and T_0^{OCL} (dashed curve, right axis) against temperature in the presence of the carrier-density-dependent internal loss. The dash- dotted curve shows T_0^{OCL} in the absence of such a loss.

T_0^{OCL} in the presence of the carrier-density-dependent internal loss (the dashed curve in Fig. 6) is also reduced compared to that in the absence of such a loss (the dash-dotted urve), which is again in contrast to the effect of charge neutrality violation in QDs. Due to the latter, T_0^{OCL} was increased [6]. A non-monotonic behavior of T_0^{OCL} with temperature should also be noted in the presence of the carrier-density-dependent internal loss. This behavior is controlled by the competition of the sum of the first two terms in eq. (13) with the last term. The sum of the first two terms presents the reciprocal of T_0^{OCL} in the absence of the carrier-density-dependent internal loss and decreases with temperature (the dash-dotted curve), the last term is introduced by the carrier-density-dependent internal loss and increases with temperature. At a certain value of the temperature, T^{max}, the third term increases infinitely since T_0^{QD} goes to zero. Hence, T_0^{OCL} goes to zero too at $T = T^{max}$.

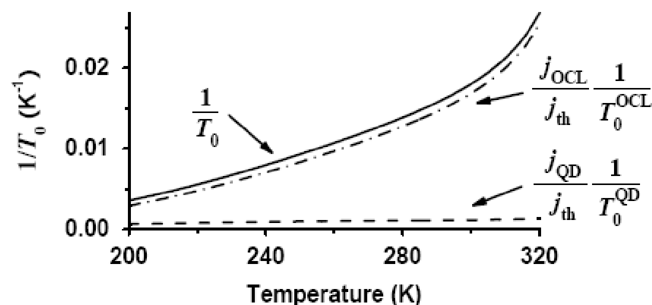

Fig. 7.

Reciprocal of T_0 and the first and the second terms in the right-hand side of eq. (4) against temperature.

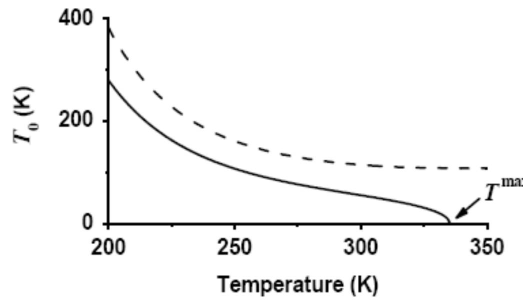

Fig.8. Characteristic temperature against temperature calculated including (solid curve) and neglecting (dashed curve) the carrier-density-dependent internal loss.

Fig.7 hows the reciprocal of T_0 and the first and second terms in the right-hand side of eq. (4). As seen from the figure, for the entire temperature range shown, $1 / T_0$ is mainly controlled by the second term. Even at low temperature, when j_{QD}/j_{th} is close to unity

and hence much larger than j_{OCL}/j_{th} ,T_0^{QD} is so high that $(j_{QD}/j_{th})(1/T_0^{QD})$ is smaller than $(j_{OCL}/j_{th})(1/T_0^{OCL})$ At high temperature, j_{QD}/j_{th} is much smaller than j_{OCL}/j_{th}, and, at the same time, T_0^{QD} is still higher than T_0^{OCL} . Although the contribution of the first term in the right-hand side of eq. (4) (which is entirely due to the carrier-density-dependent internal loss) into T_0 is minor compared to that of the second term, the latter itself is strongly modified by the carrier-density-dependent internal loss (formally through T_0^{QD}).

Hence *T*0 is considerably reduced due to such a loss. This is explicitly shown in Fig. 8 depicting the characteristic temperature *T*0 against the temperature in the presence and in the absence of carrier-density-dependent internal loss. At room temperature, T_0 is about twice as low as that neglecting such a loss.

With eqs. (4), (6) and (11)–(13), the characteristic temperature of a QD laser in the presence of carrier-density-dependent internal loss can be calculated and analyzed versus the parameters of the structure (Fig. 9).

The maximum gain $g^{\max}$ is a function of the RMS of QD size fluctuations δ and the surface density of QDs *N*S ($g^{\max} \propto NS / \delta$). As seen from (8), varying $g^{\max}$ affects *f*n and *n* and hence the temperature characteristics of a laser. The greater δ or the smaller *N*S (i.e., the smaller is $g^{\max}$), the lower is T_0 [Figs. 9(a) and (b)]. In the presence of the carrier-density-dependent internal

loss, T_0 decreases with increasing δ or decreasing *N*S faster than that neglecting such a loss [Figs. 9(a) and (b)]. While *T*0 in the absence of the carrier-density-dependent internal loss remains nonvanishing (though low) with increasing δ (or decreasing *N*S), T_0 in the presence of such a loss turns to zero at the critical value $\delta = \delta^{max}$ (or $NS = NS^{min}$). *T*0 reduces with decreasing cavity length *L* [Fig. 9(c)]. *T*0 in the absence of the carrier density- dependent internal loss remains nonvanishing with decreasing *L* while that in the presence of such a loss turns to zero at $L = L^{min}$.

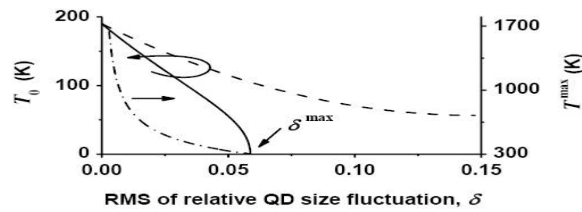

(a)

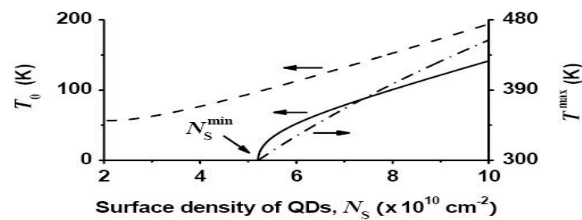

(b)

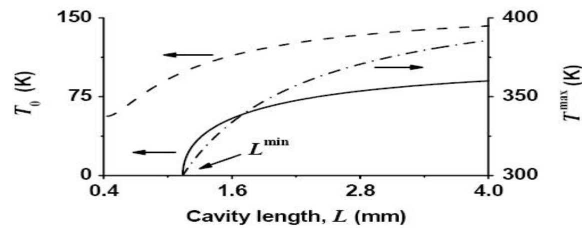

(c)

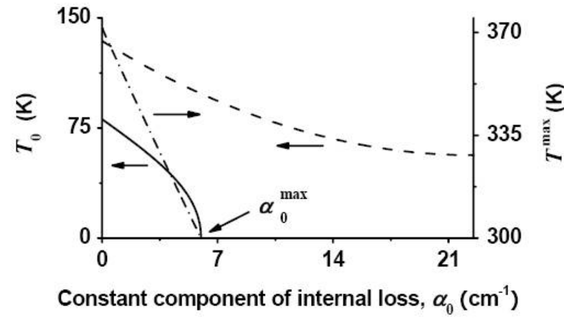

(d)

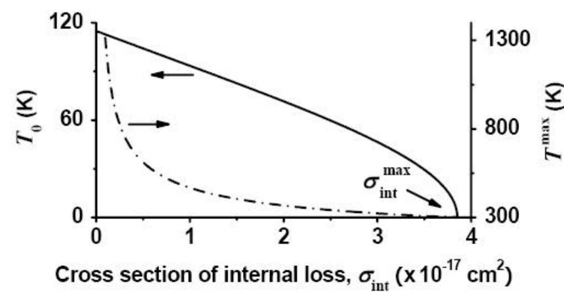

(e)

Fig.9. Characteristic temperature calculated including (solid curve, left axis) and neglecting (dashed curve, left axis) the carrier-density-dependent internal loss, and maximum operating temperature (dash-dotted curve, right axis) against RMS of QD size fluctuations (a), surface density of QDs (b), cavity length (c), constant component of internal loss (d), and cross section of internal loss (e).

Although α_0 and σ_{int} are not easily controllable parameters in a given structure, in order to illustrate their effects on T_0, we also present here the dependence on α_0 and σ_{int} [Figs. 9(d) and e)]. As seen from eq. (9), the constant component α_0 of the internal loss does not introduce any temperature dependence in *f*n and acts similarly to the mirror loss β . T_0 decreases with increasing α_0 or σ_{int}; at the critical value $\alpha_0 = \alpha_0^{max}$ or $\sigma_{int} = \sigma_{int}^{max}$, T_0 becomes zero.

As our calculations suggest, the characteristic temperature depends critically on the parameters of the laser structure. At the same time, when the parameters are far from their critical tolerable values, T_0 can be above 100 K, which is in agreement with the experimental data for properly optimized structures (see, e.g., [7–8]).

It can be seen from Fig. 9 that, as $\delta \rightarrow 0$, $L \rightarrow \infty$, $\alpha_0 \rightarrow 0$, or $\sigma_{int} \rightarrow 0$, the characteristic temperature remains finite. On the contrary, the characteristic

temperature goes to infinite with *N*S $\rightarrow \infty$. These tendencies are discussed in more detail in Appendix 2.
Eq. (4), where T_0^{QD} and T_0^{OCL} are given by eqs. (12) and (13), respectively, is the general expression for T_0 . The asymptotic expressions for T_0 when the parameters are near and far from their critical tolerable values .

V. Critical parameters controlled by the carrier-density-dependent internal loss

A. Maximum operating temperature

The characteristic temperature falls off profoundly with increasing temperature *T* (Fig.8).At a certain temperature $T^{\max}$, presenting the maximum operating temperature of the device ($T^{\max}$ = 335 K for the specific case considered here), T_0 goes to zero. Hence even in the absence of heating effects, the carrier-density-dependent internal loss itself sets an upper limit for operating temperatures of a QD laser. The point is that, the carrier density in the OCL, *n*, and hence the internal loss, $\alpha_{\text{int}} = \alpha_0 + \sigma_{\text{int}}\, n$, increase continuously with temperature. At the same time, the maximum gain of a laser can not exceed $g^{\max}$ [see eq. (8)]. For $T > T^{\max}$, the lasing condition in eq. (8) can not be satisfied. The following transcendental equation is derived for $T^{\max}$:

$$\frac{1}{\left(T^{\max}\right)^{3/4}} \exp\left(\frac{E_n}{2T^{\max}}\right) = \frac{\sqrt{2\left(m_c^{\text{OCL}}/2\pi\hbar^2\right)^{3/2}\sigma_{\text{int}}}}{\sqrt{2g^{\max}} - \sqrt{g^{\max} + \beta + \alpha_0}}. \qquad (14)$$

$T^{\max}$ is shown versus the structure parameters in Fig.9. The greater δ or the smaller *N*S
(i.e., the smaller is $g^{\max}$), the lower is $T^{\max}$ [Figs. 9(a) and (b)]. As $\delta \rightarrow 0$ or *N*S $\rightarrow \infty$, $g^{\max}$ becomes infinitely high and $T^{\max} \rightarrow \infty$ [see eq. (14) and Figs. 9(a) and (b)].
reduces with decreasing cavity length *L* [Fig. 9(c)]. As $L \rightarrow \infty$, i.e., $\beta \rightarrow 0$ $T^{\max}$, $T^{\max}$ remains finite [also see eq. (14)].
decreases with increasing α_0 or σ_{int} . Like with $g^{\max} \rightarrow \infty$, $T^{\max}$ becomes $T^{\max}$ infinitely high when $\sigma_{\text{int}} \rightarrow 0$ [Fig. 9(e) and eq. (14)]. This tendency is readily

seen also from eq. (8) — if $\sigma_{\text{int}} \rightarrow 0$ (α_{int} becomes temperature-independent: $\alpha_{\text{int}} \rightarrow \alpha_0$) or $g^{\max} \rightarrow \infty$, the solution for *f*n exists at any temperature *T*.

In the presence of the carrier-density-dependent internal loss, the critical tolerable parameters depend on temperature. In Fig. 9, room-temperature values of the critical parameters are used. That is why when any of the

parameters (δ, *N*S, *L*, α_0, or σ_{int}) approaches its critical value ($\delta^{\max}$, $L^{\max}$, $Ns^{\min}$, $\alpha_0^{\max}$, or $\sigma_{\text{int}}^{\max}$, respectively), $T^{\max}$ reduces to 300 K. Beyond the critical tolerable value of any parameter, $T^{\max}$ goes below 300 K, i.e., no room-temperature lasing is possible.

B. Shallowest potential well depth and smallest tolerable size of a QD

The carrier density *n* in the OCL [eq. (6)] is also strongly controlled by the excitation
energy E_n from a QD. The smaller E_n, the easier for carriers to escape to the OCL and hence the higher are *n* and α_{int}. Just as $T^{\max}$ exists, there is a lowest excitation energy, $E_n^{\min}$, below which no lasing is attainable in a structure. From eq. (14), an explicit expression is apparent for $E_n^{\min}$,

$$E_n^{\min} = T \ln\left[\frac{\sigma_{\text{int}} N_c^{\text{OCL}}}{\left(\sqrt{2g^{\max}} - \sqrt{g^{\max} + \beta + \alpha_0}\right)^2}\right]. \qquad (15)$$

For $E_n^{\min} < E_n$, the thermal escapes from QDs to the OCL will be so intensive that the population inversion required for the lasing can not be attained.
Since E_n decreases with reducing QD size [E_n is the separation between the quantized

energy level and the top of the well — see the inset in Fig. 10(a)], there also exists the smallest tolerable QD size $a^{\min}$. It has been known (see, e.g., [9]) that, in contrast to one-dimensional symmetrical potential well (which supports the quantized energy level no matter how thin it is), there is a smallest size of a three-dimensional (even symmetrical) well (QD), beyond which no bound state can

exist. As seen from the present analysis, a more strict condition should be satisfied to attain lasing in the presence of the carrier-density-dependent internal loss. Just having a confined energy level in a QD is not sufficient — the level should be so deeply localized that the carrier density in the OCL and the internal loss are low enough for holding the lasing condition eq. (8).

Figure 10 shows the minimum tolerable excitation energy $E_n^{\min}$ as a function of the structure parameters. As also readily seen from eq. (15), $E_n^{\min}$

decreases with decreasing RMS relative QD size fluctuations δ [Fig. 10(a)], increasing surface density of QDs *N*S [Fig. 10(b)], increasing cavity length *L* [Fig. 10(c)], decreasing constant component of internal loss α_0 [Fig. 2.9(d)], or reducing cross section of internal loss σ_{int} [Fig. 10(e)]. At certain values $g^{\max}$ (i.e., certain values of δ or *N*S, since $g^{\max} \propto Ns / \delta$ [7]) or σ_{int} given by

$$\left(g^{\max}\right)^* = \left(\sqrt{2\sigma_{\text{int}} N_c^{\text{OCL}}} + \sqrt{\sigma_{\text{int}} N_c^{\text{OCL}} + \beta + \alpha_0}\right)^2, \qquad (16)$$

$$\sigma_{\text{int}}^* = \frac{\left(\sqrt{2g^{\max}} - \sqrt{g^{\max} + \beta + \alpha_0}\right)^2}{N_c^{\text{OCL}}}, \qquad (17)$$

the minimum tolerable excitation energy turns to zero, $E_n^{\min} = 0$. On further increasing $g^{\max}$ (i.e., decreasing δ or increasing *N*S) or further decreasing σ_{int}, eq. (15) would formally give negative $E_n^{\min}$. Hence, for $g^{\max} \geq (g^{\max})^*$ (i.e., $\delta \leq \delta^*$ or $Ns \geq Ns^*$) or $\sigma_{\text{int}} \leq \sigma_{\text{int}}^*$, the restriction placed by the carrier-density-dependent internal loss on the shallowest potential well depth or the smallest QD size is removed — the minimum size is solely determined by the condition of existence of a bound state. For a specific structure considered here, $(g^{\max})^* =$ 74.64 cm^{-1} (i.e., $\delta^* = 0.02$ or $Ns^* = 1.54\times10^{11}\ cm^{-2}$),
and $\sigma_{\text{int}} = 0.57 \times 10^{-17}\ cm^{-2}$.

Since $E_n^{\min}$ depends on the structure parameters, so does $a^{\min}$. The smaller β (the longer *L*), α_0 or δ , or the larger *N*S, the smaller is $a^{\min}$.

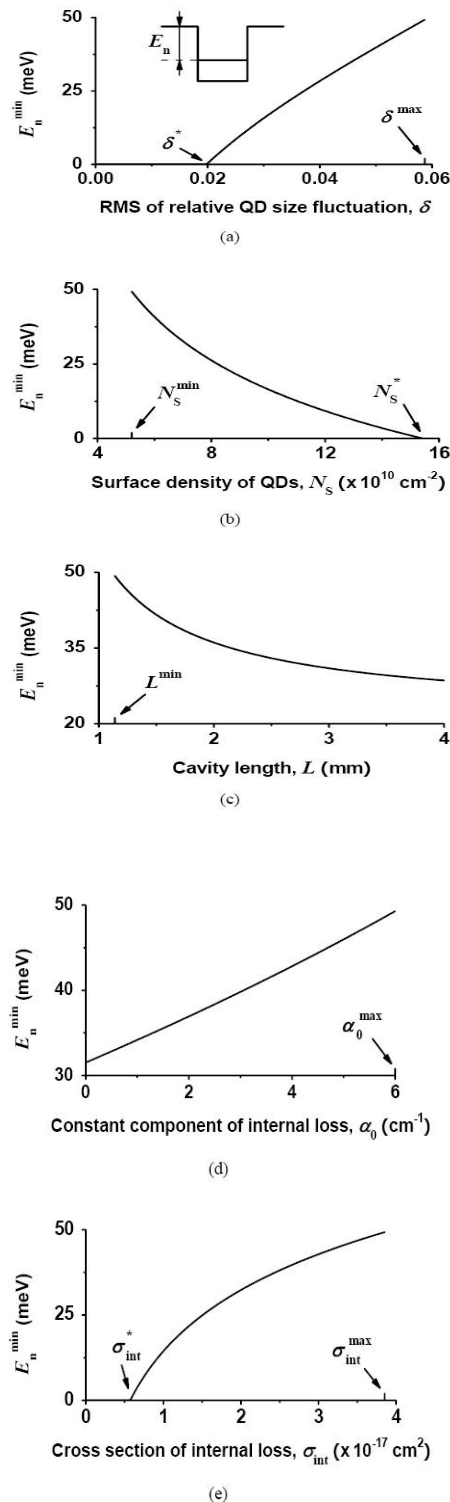

Fig. 10. Minimum tolerable excitation energy from a QD against RMS of QD size fluctuations (a), surface density of QDs (b), cavity length (c), constant component of internal loss (d), and cross section of internal loss (e). The inset in (a) shows schematically the potential well of a QD and the excitation energy E_n .

As shown previously [9, 8,9] there exist the critical tolerable values of the parameters of a QD structure beyond which no lasing is attainable. These critical quantities are the maximum RMS of QD-size fluctuations $\delta^{\max}$, the minimum surface density of QDs $Ns^{\min}$ the minimum cavity length $L^{\min}$, and the maximum cross-section of internal loss $\sigma_{\text{int}}^{\max}$. As shown here, there are three more critical parameters ($T^{\max}$, $E_n^{\min}$, and $a^{\min}$) in the presence of the carrier-density dependent internal loss

VI. Conclusion

A detailed theoretical analysis has been carried out on the temperature dependence of the threshold current density of a semiconductor QD laser in the presence of the carrier- density dependent internal optical loss in the waveguide (OCL). In the presence of such a loss, the confined-carrier level occupancy in QDs is coupled to the free-carrier density in the OCL by the threshold condition. Due to this coupling, the free-carrier density is increased and more temperature-sensitive, and also the confined-carrier level occupancy becomes temperature - dependent. As a result, the characteristic temperature of a laser is considerably reduced; at room temperature, for a specific structure considered in this paper, T_0 is about twice as low as that neglecting the internal loss. Carrier-density-dependent internal loss also sets an upper limit for the operating temperatures of a QD laser and constrains the shallowest potential well depth and the smallest tolerable size of a QD at which the lasing can be attained. The dependences of the characteristic temperature, maximum operating temperature, and shallowest potential well depth on the parameters of the structure are obtained. At the maximum operating temperature or when any parameter of the structure is equal to its critical tolerable value, the characteristic temperature reduces to zero.

REFERENCES

[1] L. V. Asryan and R. A. Suris, "Longitudinal spatial hole burning in a quantum-dot laser," *IEEE J. Quantum Electron.*, vol. 36, no. 10, pp. 1151–1160, Oct. 2000.
[2] M. V. Maximov, L. V. Asryan, Yu. M. Shernyakov, A. F. Tsatsul'nikov, I. N. Kaiander, V.V. Nikolaev, A. R. Kovsh, S. S. Mikhrin, V. M. Ustinov, A. E. Zhukov, Zh. I. Alferov, N.N. Ledenstov, and D. Bimberg, "Gain and threshold characteristics of long wavelength lasers based on InAs/GaAs quantum dots formed by activated alloy phase separation," *IEEE J. Quantum Electron.*, vol. 37, no. 5, pp. 676–683, May 2001.
[3] O. B. Shchekin and D. G. Deppe, "1.3 μm InAs quantum dot laser with *T*0 = 161 K from 0 to 80 °C," *Appl. Phys. Lett.*, vol. 80, no. 18, pp. 3277–3279, May 2002.
[4] A.R. Kovsh, N.A. Maleev, A.E. Zhukov, S. S. Mikhrin, A.P. Vasil'ev, Yu. M. Shernyakov, M.V. Maximov, D. A. Livshits, V.M. Ustinov, Zh. I. Alferov, N. N. Ledentsov, and D. Bimberg, "InAs/InGaAs/InAs quantum dot lasers of 1.3 μm range with high (88%) differential efficiency," *Electron. Lett.*, vol. 38, no. 19, pp. 1104–1106, Sep. 2002.
[5] V. Tokranov, M. Yakimov, A. Katsnelson, M. Lamberti, and S. Oktyabrsky, "Enhanced thermal stability of laser diodes with shape-engineered quantum dot medium," *Appl. Phys. Lett.*, vol. 83, no. 5, pp. 833–835, Aug. 2003.
[6] L. V. Asryan and S. Luryi, "Effect of internal optical loss on threshold characteristics of semiconductor lasers with a quantum-confined active region," *IEEE J. Quantum Electron.*, vol. 40, no. 7, pp. 833–843, July 2004.
[7] N.-H. Kim, J.-H. Park, L. J. Mawst, T. F. Kuech, and M. Kanskar, "Temperature sensitivity of InGaAs quantum-dot lasers grown by MOCVD," *IEEE Photon. Technol.Lett.*, vol. 18, no. 8, pp. 989-991, Apr. 2006.
[8] L. Jiang and L. V. Asryan, "Maximum operating temperature of quantum dot laser," *Abstracts of International Symposium and Spring School "Nano and Giga Challenges inElectronics and Photonics"*. Phoenix, Arizona, Mar. 12–16, 2007. p. 37.
[9] L. Jiang and L.V. Asryan, "Internal-loss-limited maximum operating temperature and characteristic temperature of quantum dot laser," *Laser Phys. Lett.*, vol. 4, no. 4, pp. 265– 269, Apr. 2007.
[10] L. Jiang and L.V. Asryan, "Maximum operating temperature and characteristic temperature of a quantum dot laser in the presence of internal loss," *Proceedings of SPIE's International Symposium Photonics West*. San Jose, California, Jan. 20–25 2007. vol. 6481, pp. 648107-1–648107-6.